Supplementary Information

Extending lead-free organic-inorganic semiconducting materials to new polymeric structures: 2,2'-bipyridinium iodoantimonate and quinoxalinium iodobismuthate

Chakib Hrizi,[a,*] Monia Hamdouni,[a] Marwa Essid,[a] Mourad Nouiri,[b] Abderrahim Khatyr,[c] Michael Knorr,[c] Lydie Viau,[c] Annika Schmidt,[d] Carsten Strohmann[d] and Slaheddine Chaabouni[e]

[a] Research Unit Advanced Materials, Applied Mechanics, Innovative Processes, and Environment, UR22ES04, Higher Institute of Applied Sciences and Technology of Gabes, University of Gabes, Tunisia.

[b] Laboratory of Physics of Materials and Nanomaterials Applied at Environment, Faculty of Science of Gabes, University of Gabes, Gabes, Tunisia

[c] Institut UTINAM UMR 6213 CNRS, Université Marie et Louis Pasteur, 16, Route de Gray, 25030 Besançon, France.

[d] Anorganische Chemie, Technische Universität Dortmund, Otto-Hahn Straße 6, 44227 Dortmund, Germany.

[e] Laboratoire des Sciences des Matériaux et de l'Environnement, Faculté des Sciences de Sfax, Université de Sfax, BP 1171, 3000 Sfax, Tunisia.

***Corresponding Author,** *Email: h_chakib1212@yahoo.fr*

Table of contents

References

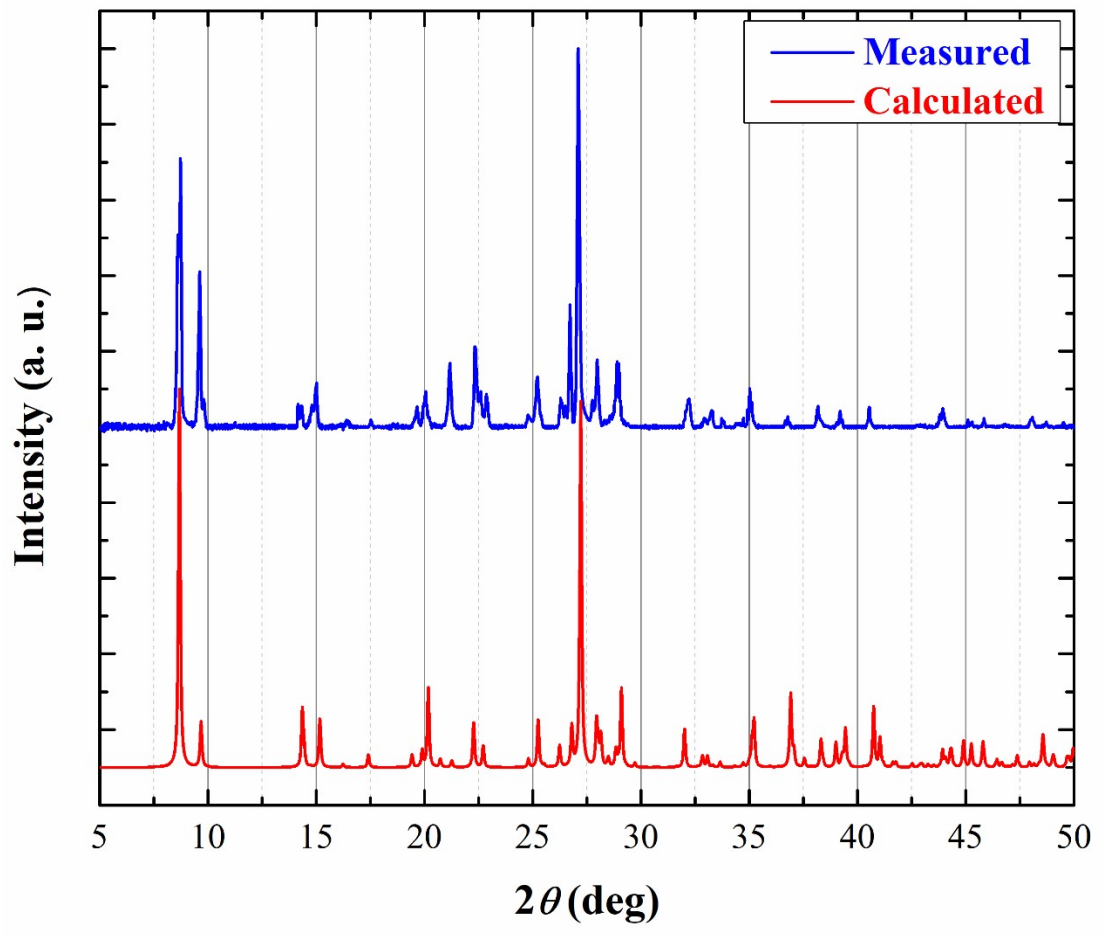

Figure S1. Comparison of the experimental PXRD pattern of (bpy-H)SbI_4 **(1)** compound with the simulated one.

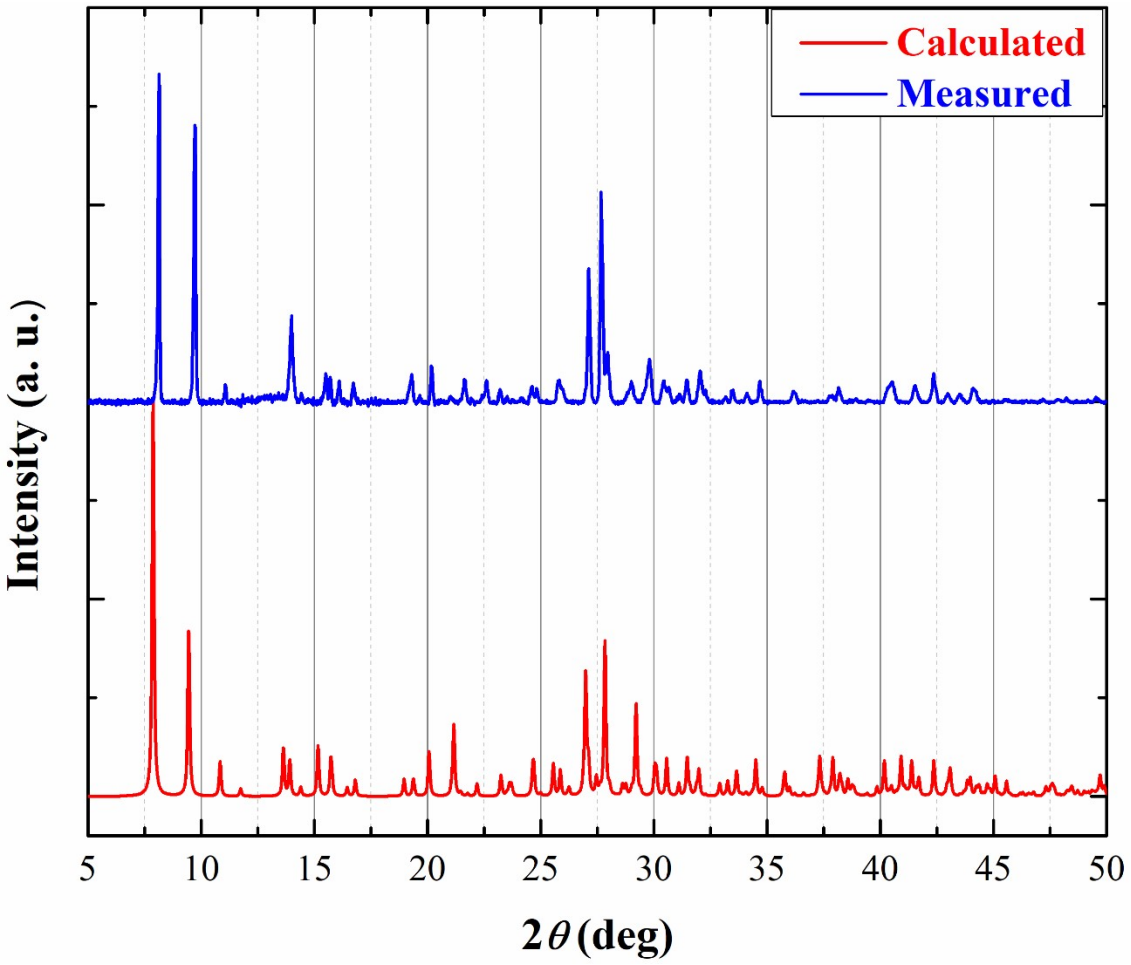

Figure S2. Comparison of the experimental PXRD pattern of $(Qx\text{-}H)_2[BiI_4]_2.CH_3OH$ **(2)** compound with the simulated one.

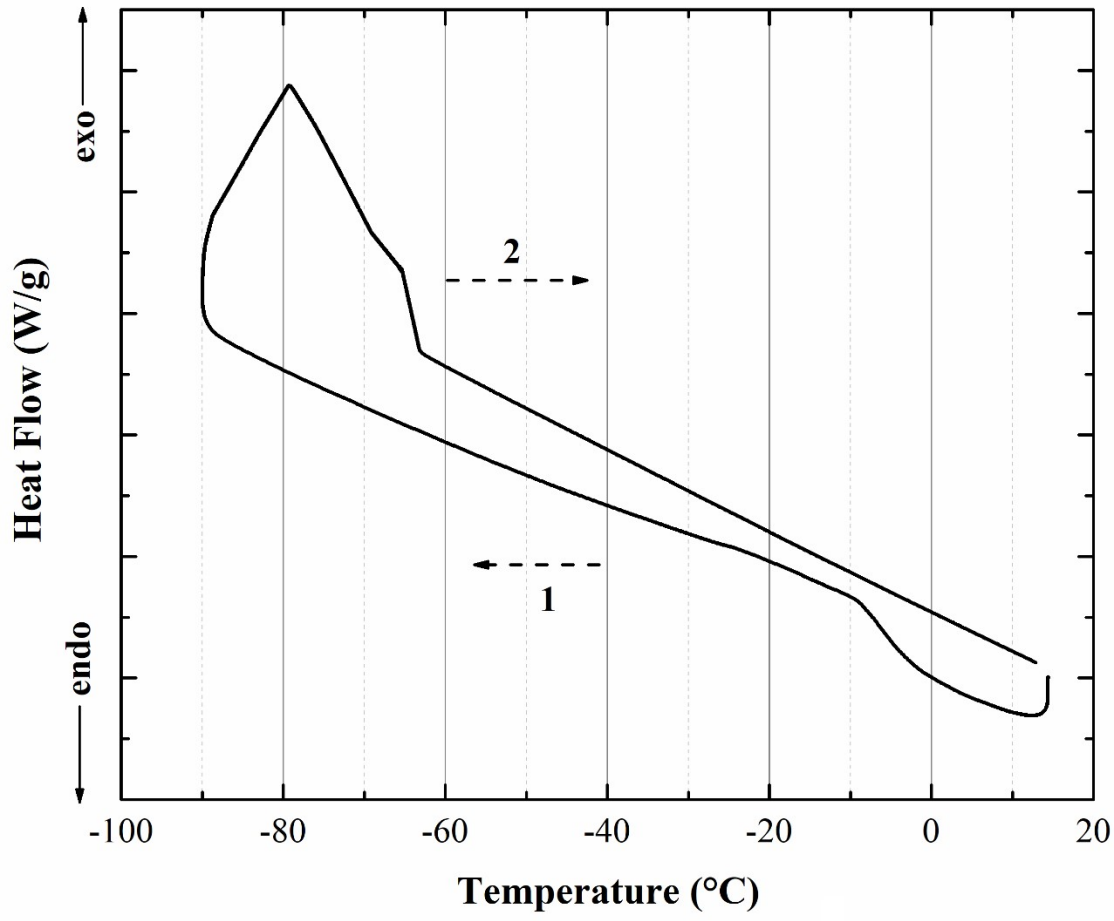

Figure S3. DSC curve for **1** at the rate of 5 °C/min upon cooling and heating.

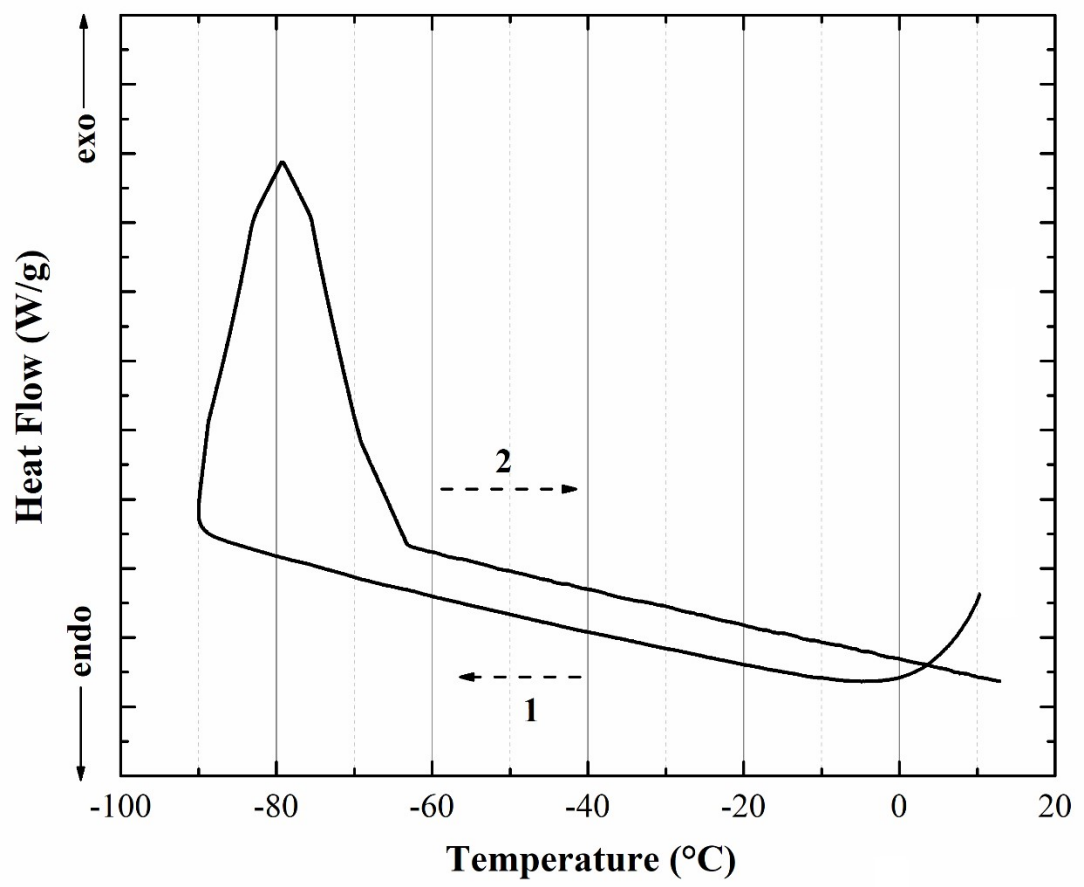

Figure S4. DSC curve for **2** at the rate of 5 °C/min upon cooling and heating.

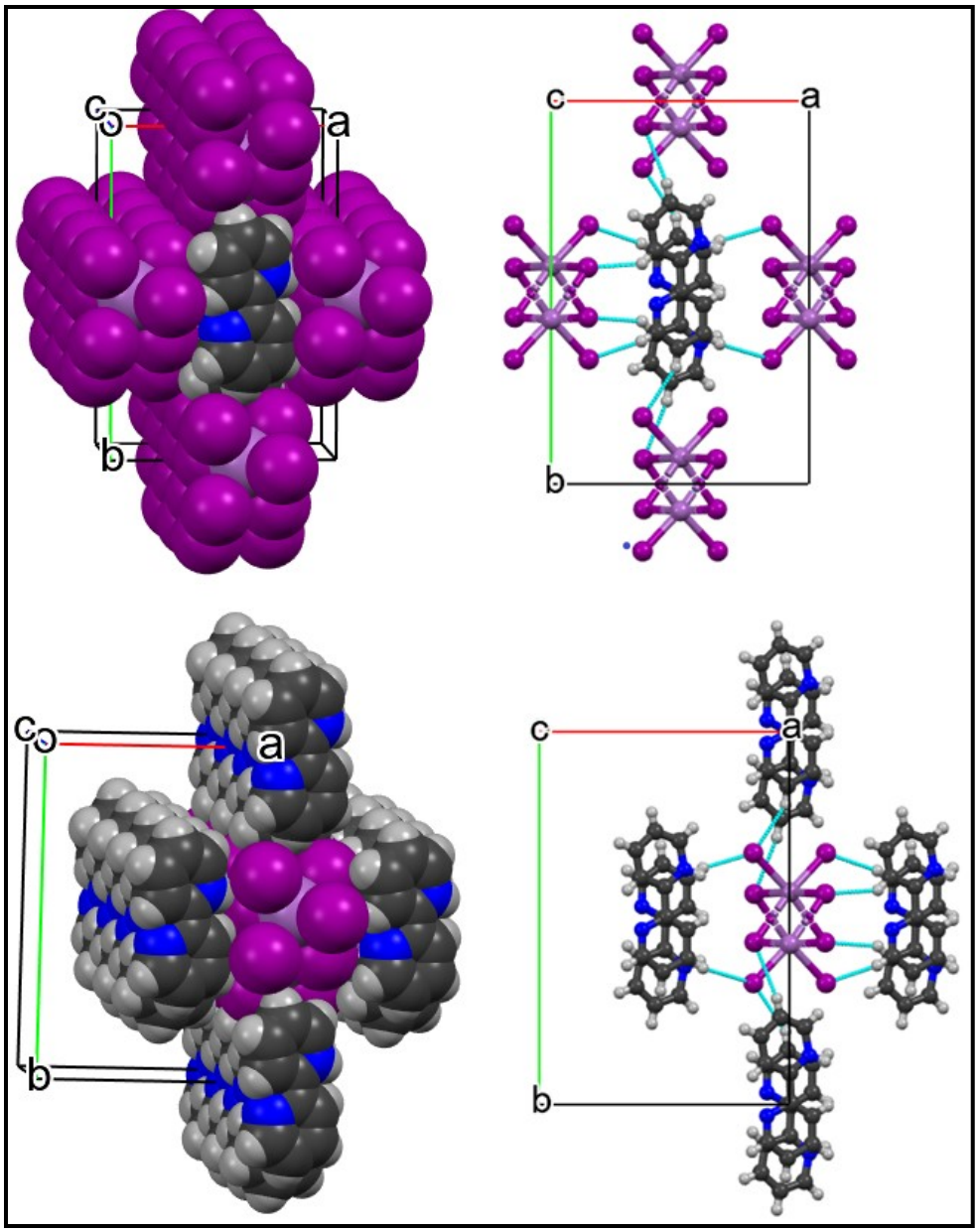

Figure S5. Illustration of H-bond contacts in compound **1** (dashed lines) between anionic 1D chains and 2,2'-bipyridinium cations showing H···I (<3.10 Å) interactions between molecular units.

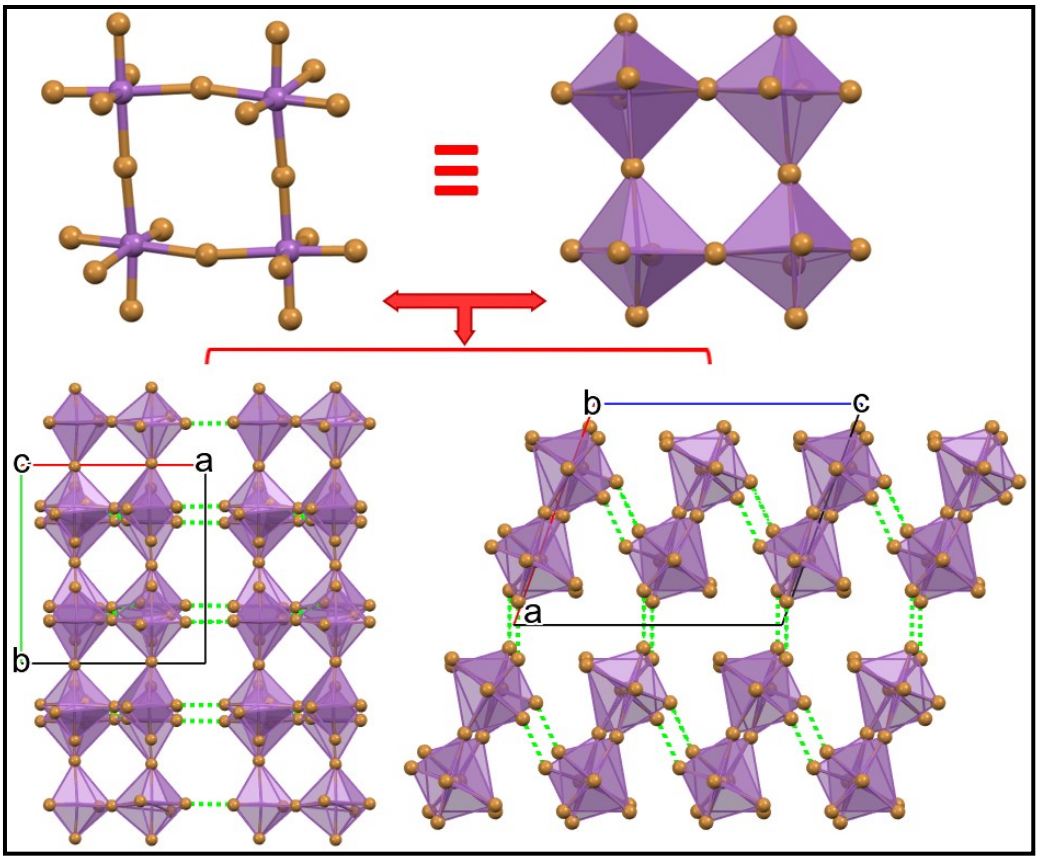

Figure S6. The crystal structure of the compounds $(2,2'\text{-Hbpy})_4Sb_4X_{20}$ (X=Br and Cl): part of the tetramer $[Sb_4X_{20}]^{8-}$; illustration of $[Sb_4X_{20}]^{8-}\cdots[Sb_4X_{20}]^{8-}$ contacts (dashed lines) between the anionic tetramers showing Br···Br (<3.92 Å) and Cl···Cl (<3.62 Å) interactions between molecular units[1,2].

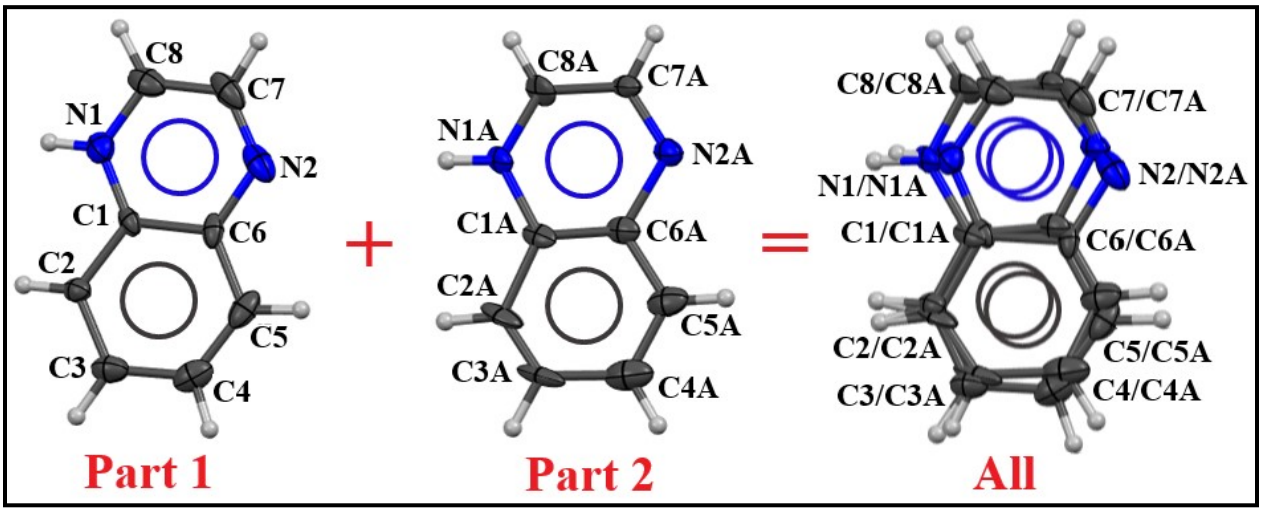

Figure S7. Disorder in quinoxalinium cation.

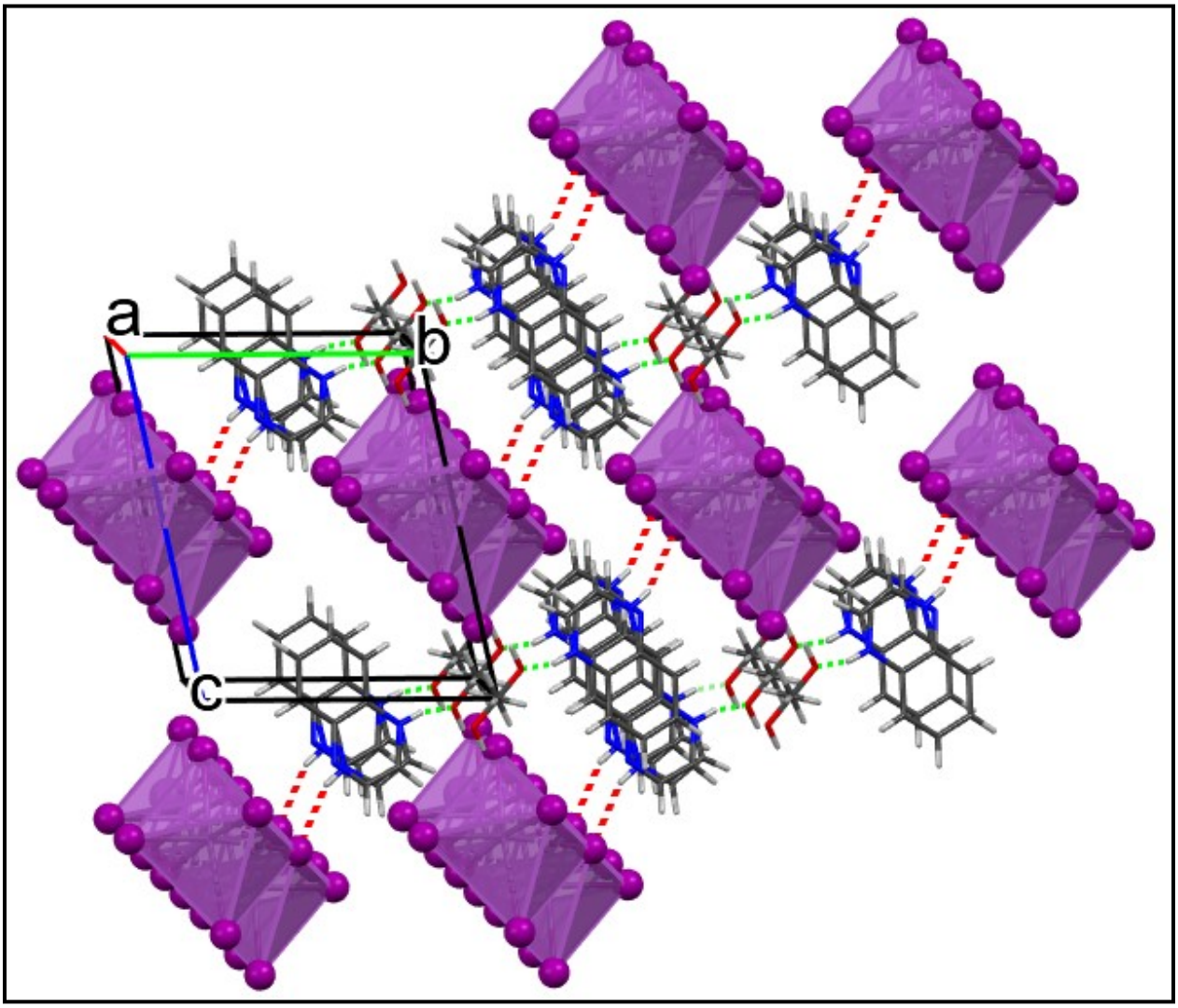

Figure S8. Illustration of H-bond contacts in compound **2** (dashed lines) between anionic 1D chains, MeOH molecules and quinoxalinium cations showing H···I and H···O (<3.10 Å) interactions between molecular units.

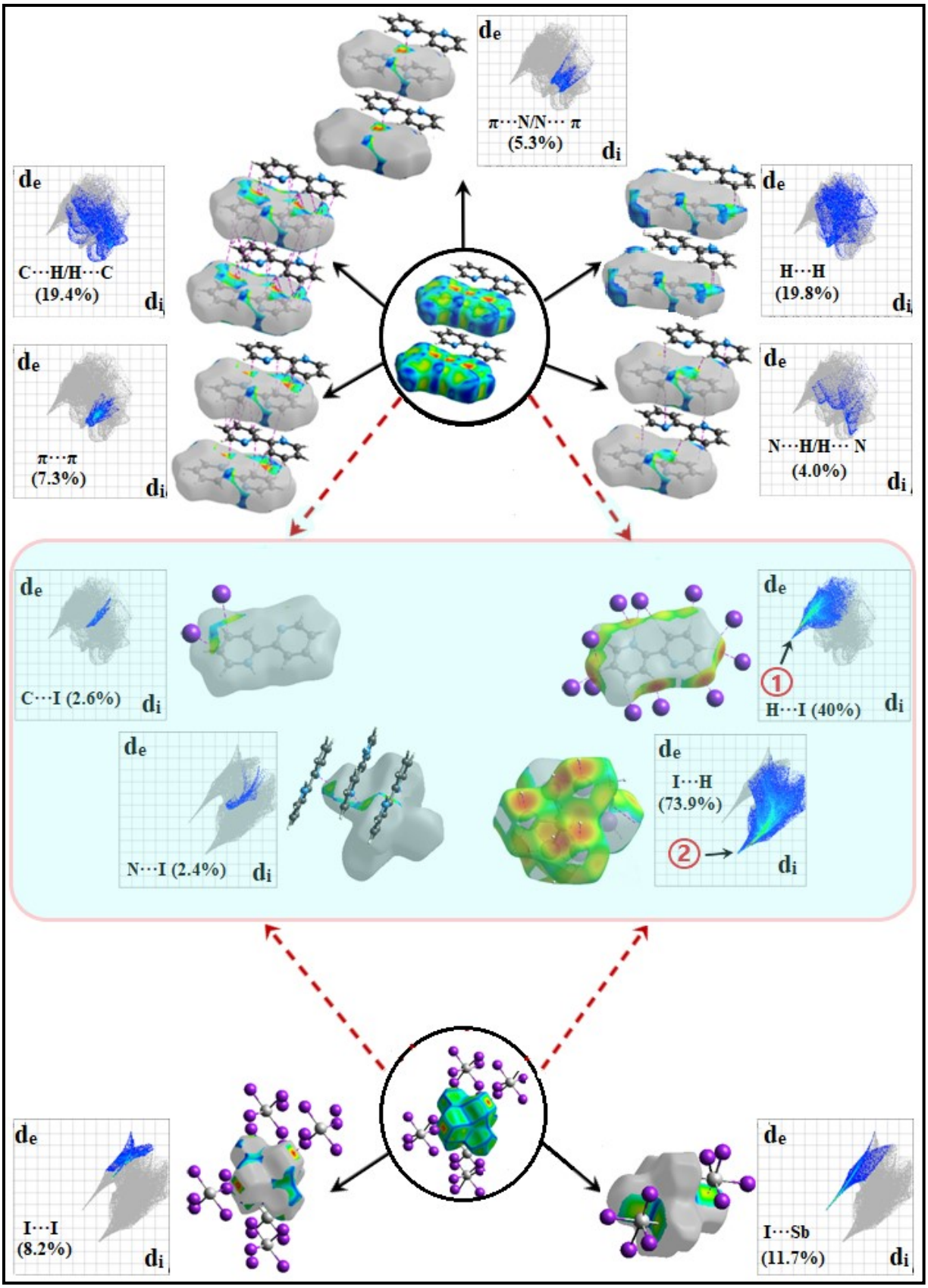
de
π···N/N··· π
(5.3%)
di
de
C···H/H···C
(19.4%)
di
de
H···H
(19.8%)
di
de
π···π
(7.3%)
di
de
N···H/H··· N
(4.0%)
di
de
C···I (2.6%)
di
de
1
H···I (40%)
di
de
N···I (2.4%)
di
de
I···H
(73.9%)
2
di
de
I···I
(8.2%)
di
de
I···Sb
(11.7%)
di

Fig. S9. Compound **1**: Decomposed Hirshfeld surfaces (mapped with d_e and shape index) and 2D-fingerprint plots resolved into defined contacts showing percentages of contacts contributed on the total Hirshfeld surface area of the molecule. The colored area in the middle shows the interactions between organic molecules and anionic units. The area above shows the interactions between organic molecules, and the area below shows the interactions between anionic units.

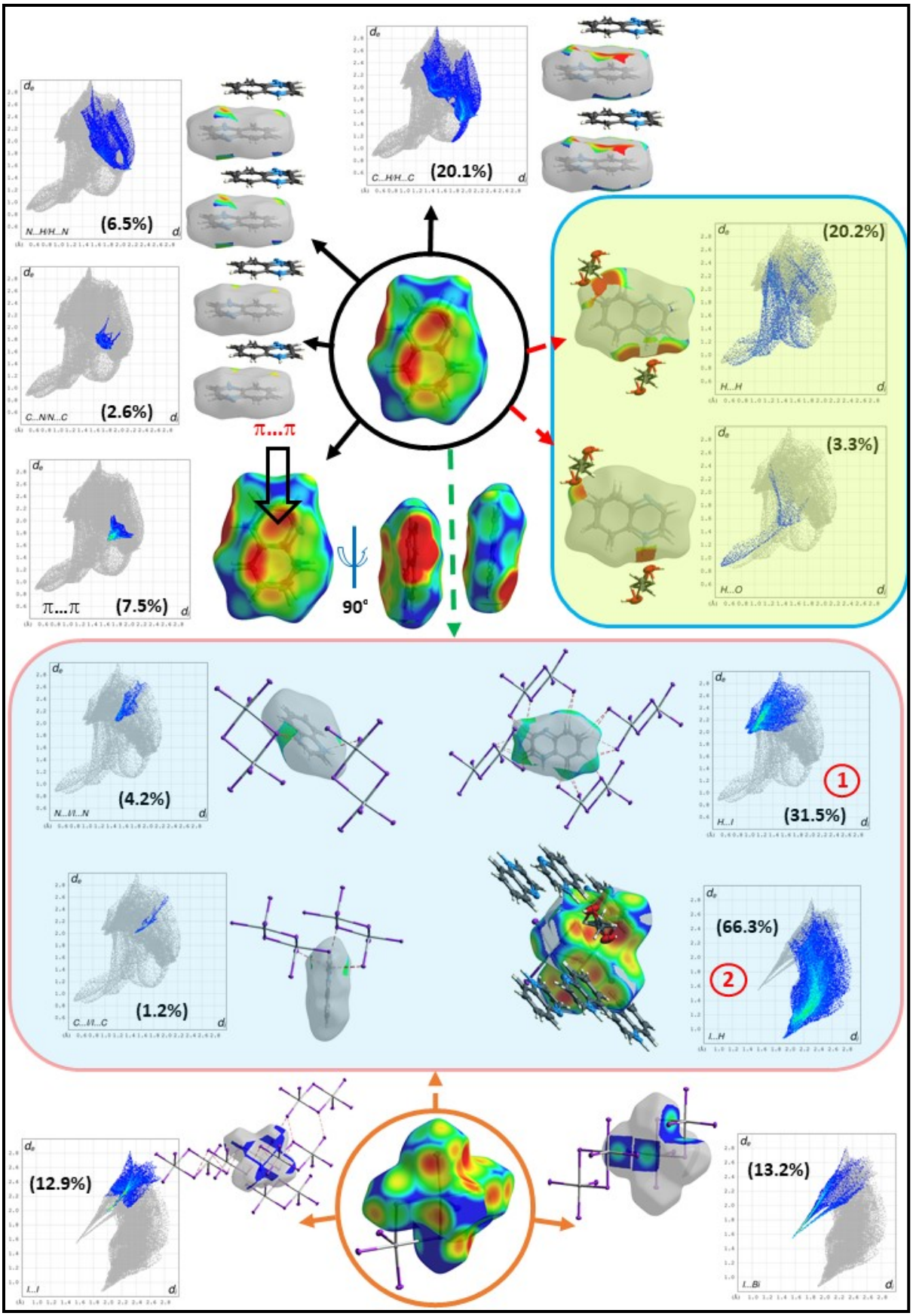
(6.5%)
(20.1%)
(20.2%)
(2.6%)
(3.3%)
π...π
(7.5%)
90°
(4.2%)
(31.5%)
(1.2%)
(66.3%)
(12.9%)
(13.2%)

Fig. S10. Compound **2**: Decomposed Hirshfeld surfaces and 2D-fingerprint plots of different interactions. The blue colored area shows the interactions between organic molecules and anionic units. The green colored area shows the interactions between organic cations and methanol molecules. The top-left HS and FP show the interactions between organic molecules. The bottom HS and FP show the interactions between anionic units.

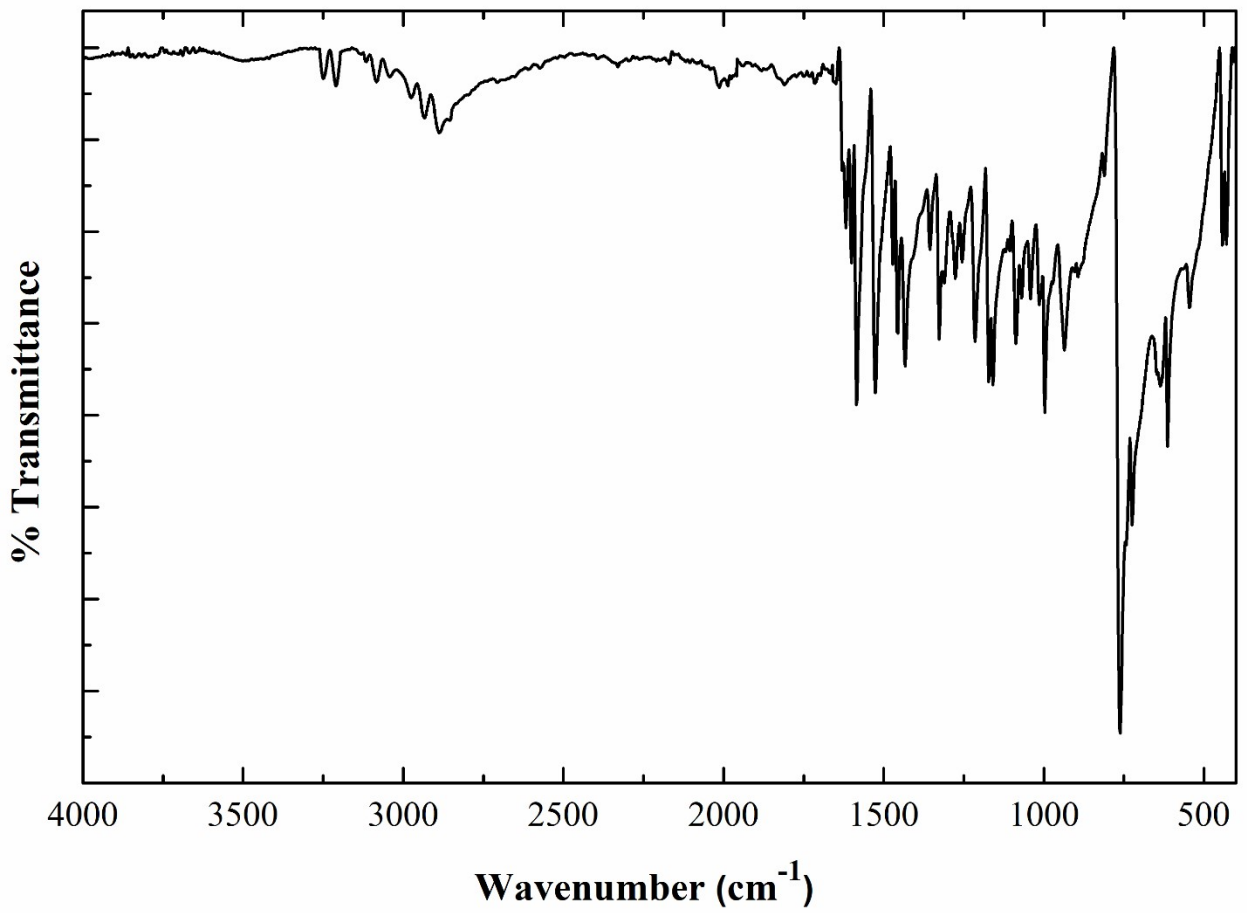

Figure S11. IR spectrum at room temperature for **1**

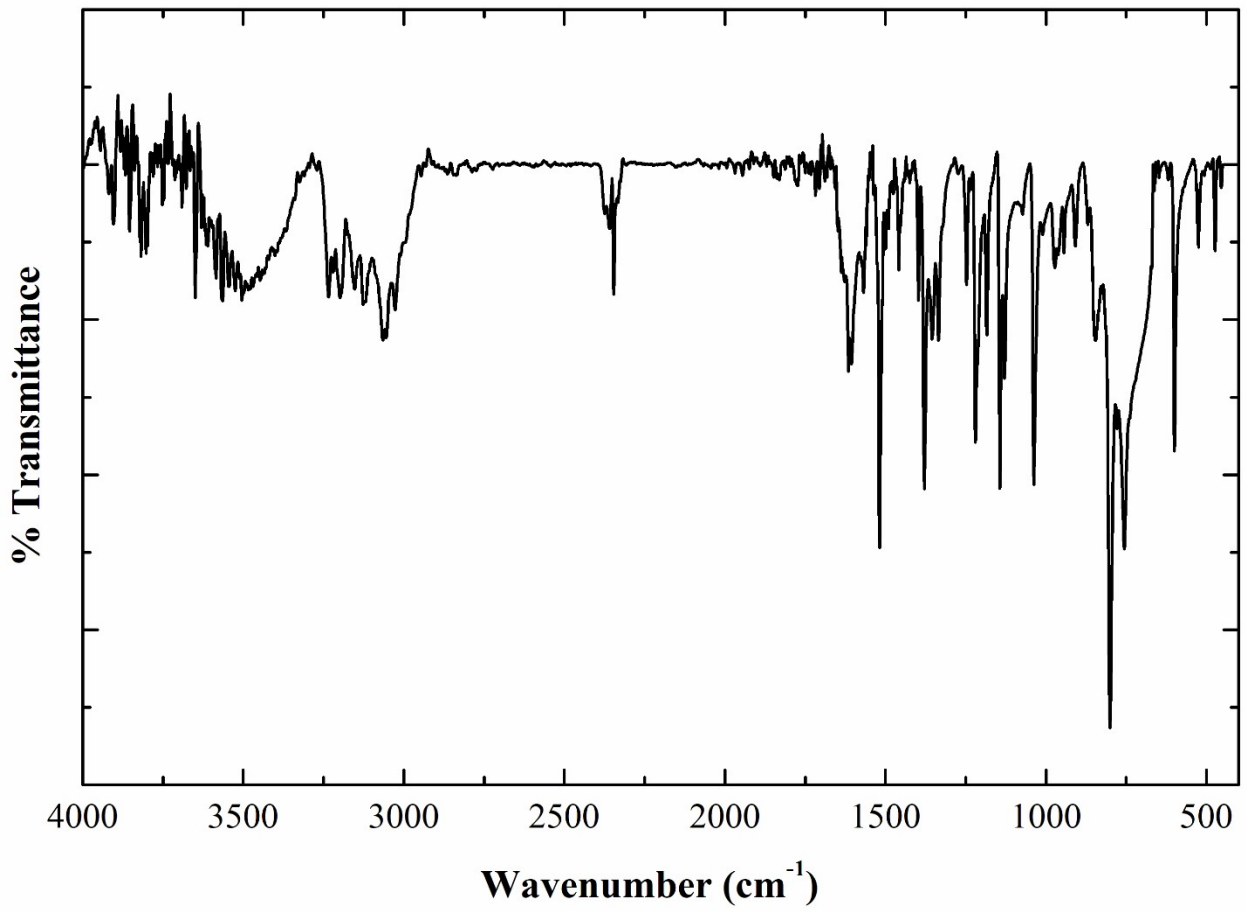

Figure S12. IR spectrum at room temperature for **2**

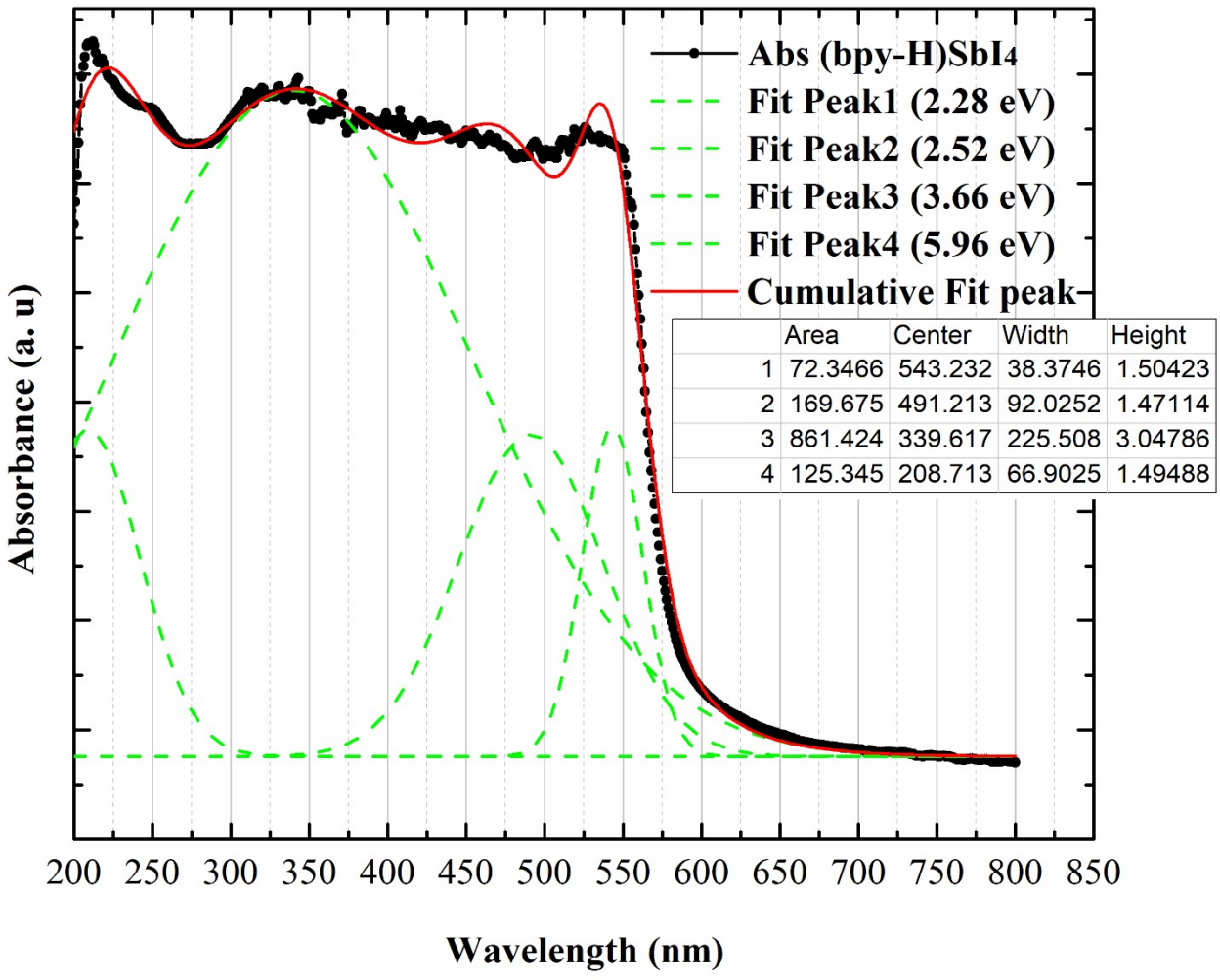

	Area	Center	Width	Height
1	72.3466	543.232	38.3746	1.50423
2	169.675	491.213	92.0252	1.47114
3	861.424	339.617	225.508	3.04786
4	125.345	208.713	66.9025	1.49488

Figure S13. UV–Vis absorption spectra for **1** measured and their Gaussian decomposition.

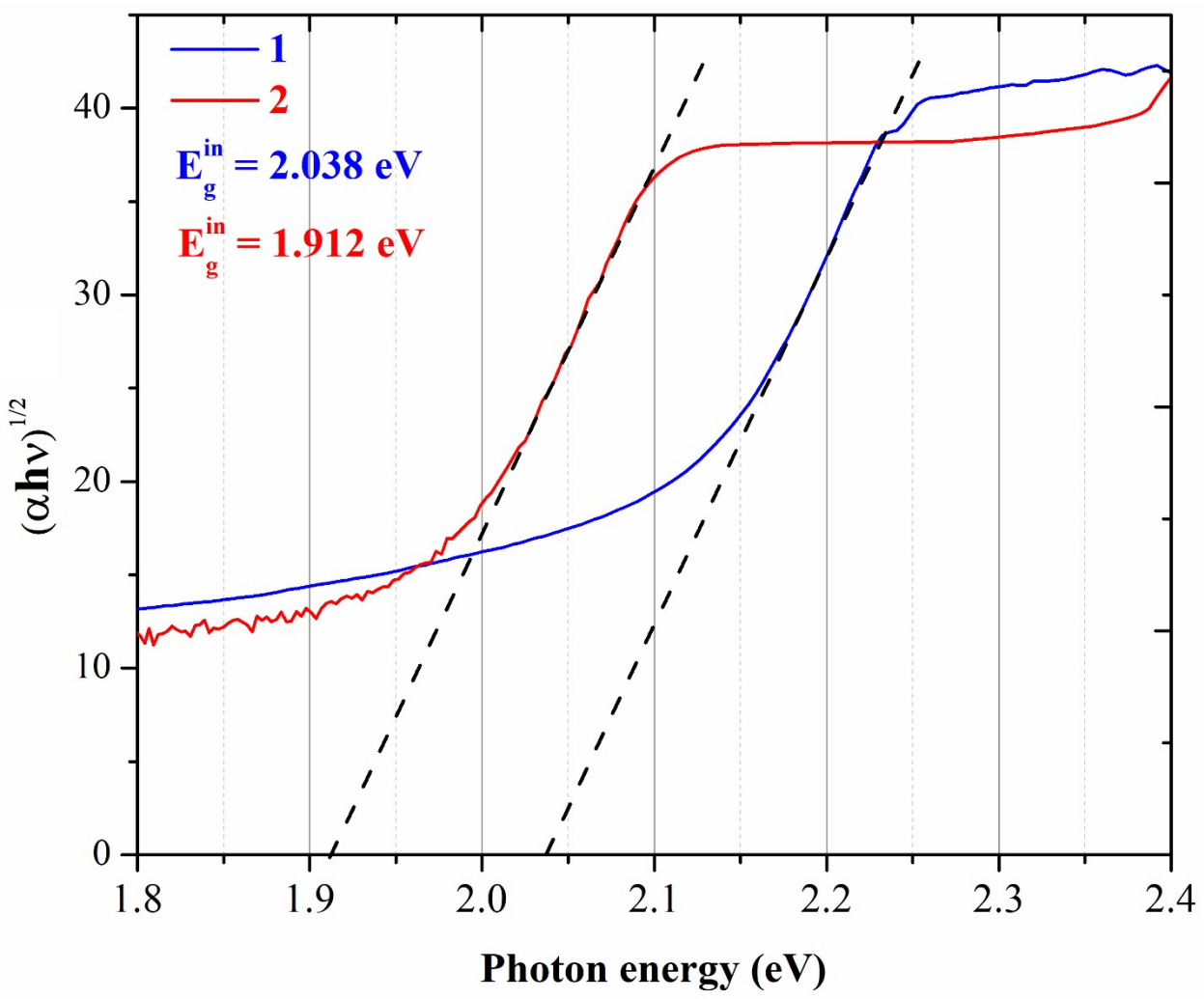

Figure S14. Tauc plots of the absorbance data for an indirect allowed transition in **1** and **2**. Fits to the linear portions of the plots give the indirect bandgaps as 2.038 eV for **1** and 1.912 eV for **2**.

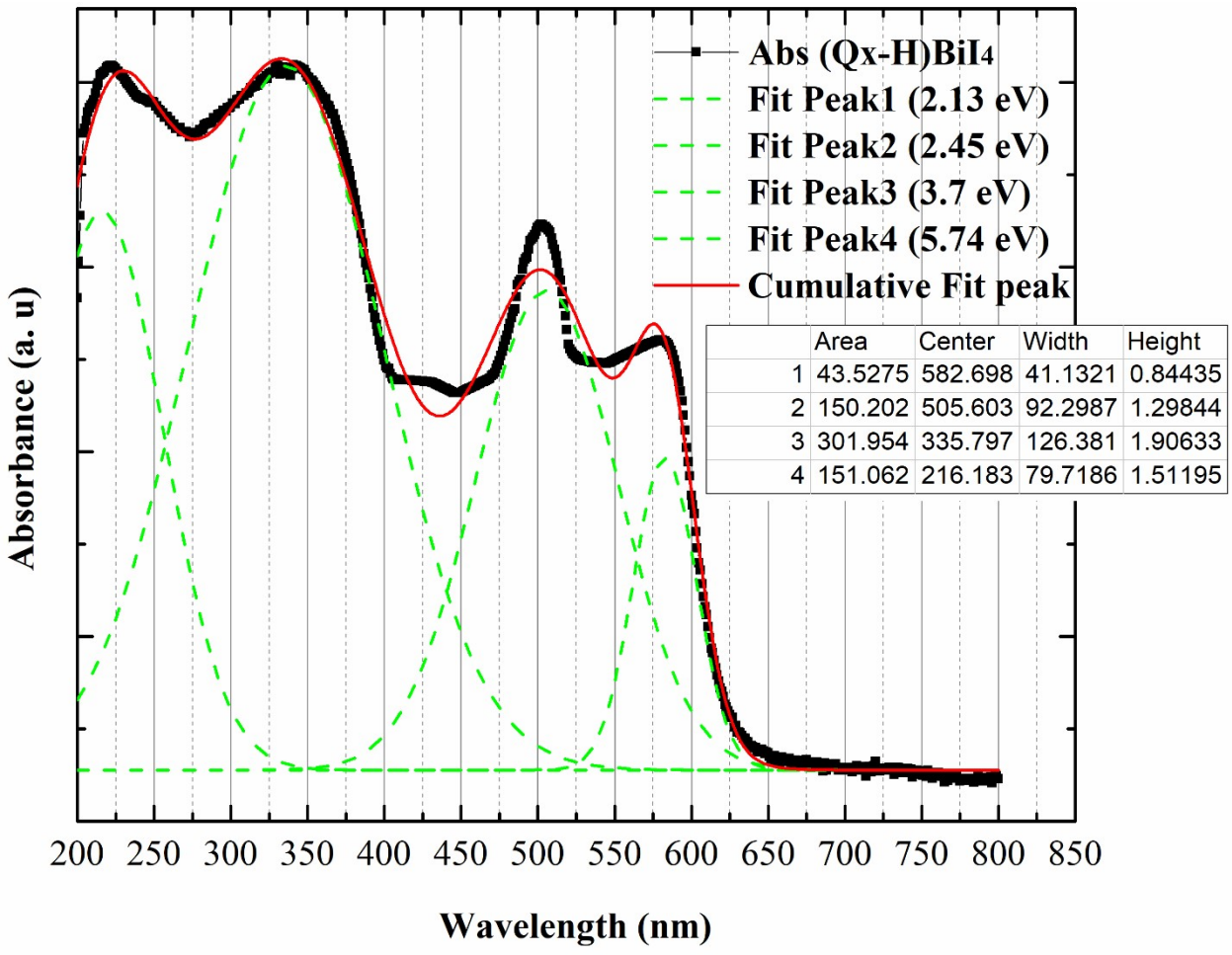

Figure S15. UV–Vis absorption spectra for **2** measured and their Gaussian decomposition.

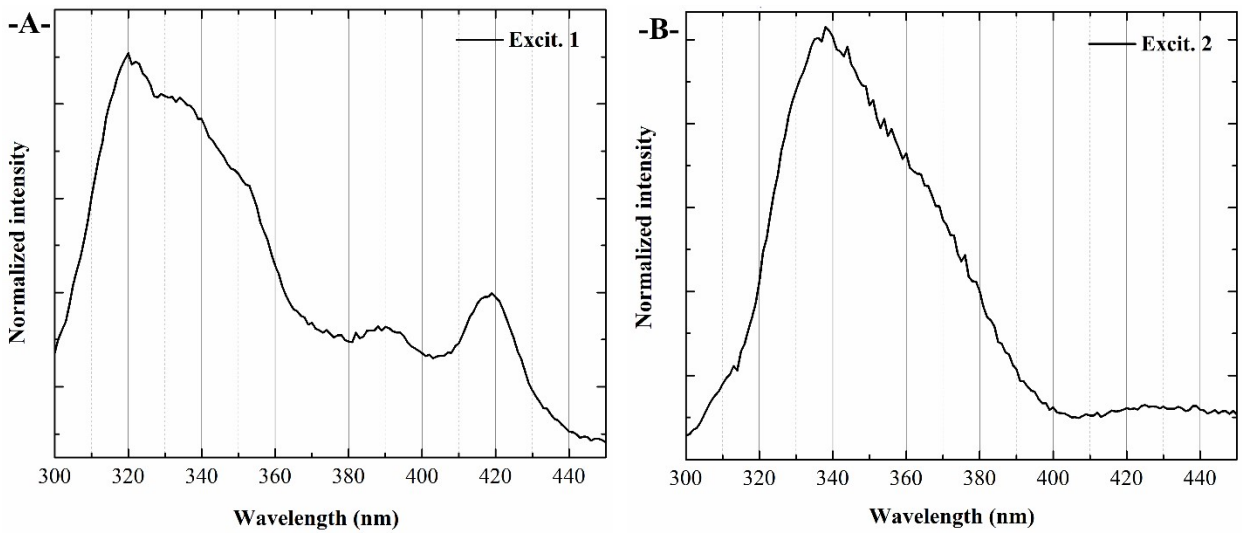

Figure S16. Normalized excitation spectra of (**A**) **1** (λ_{em} = 470 nm) and (**B**) **2** (λ_{em} = 460 nm) recorded in CH_3CN at 298 K.

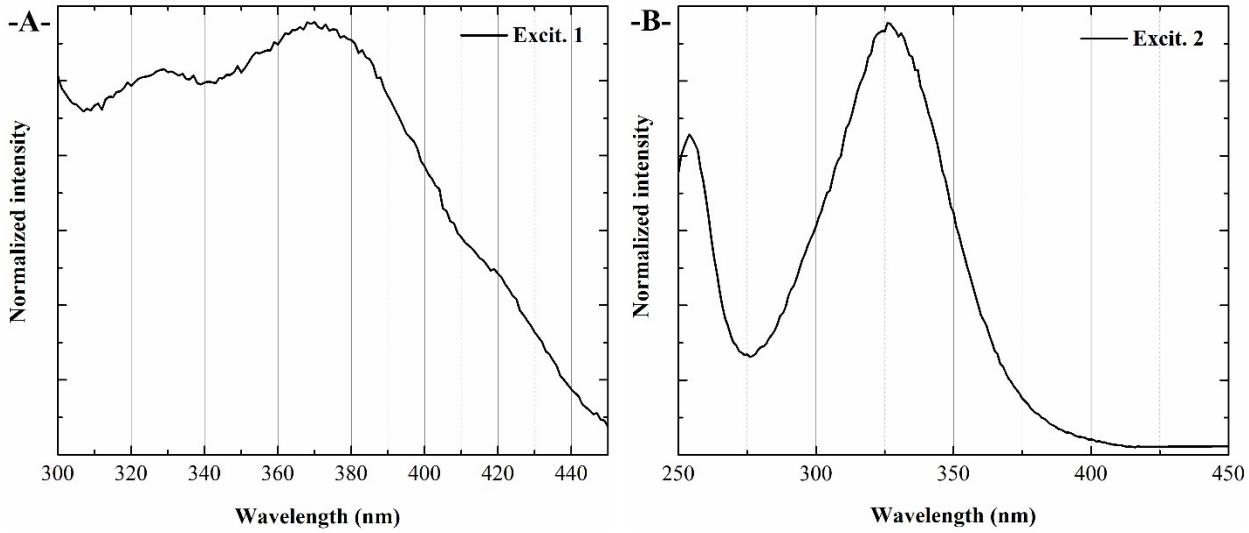

Figure S17. Normalized excitation spectra of (**A**) **1** (λ_{em} = 530 nm) and (**B**) **2** (λ_{em} = 450 nm) recorded in solid-state at 298 K.

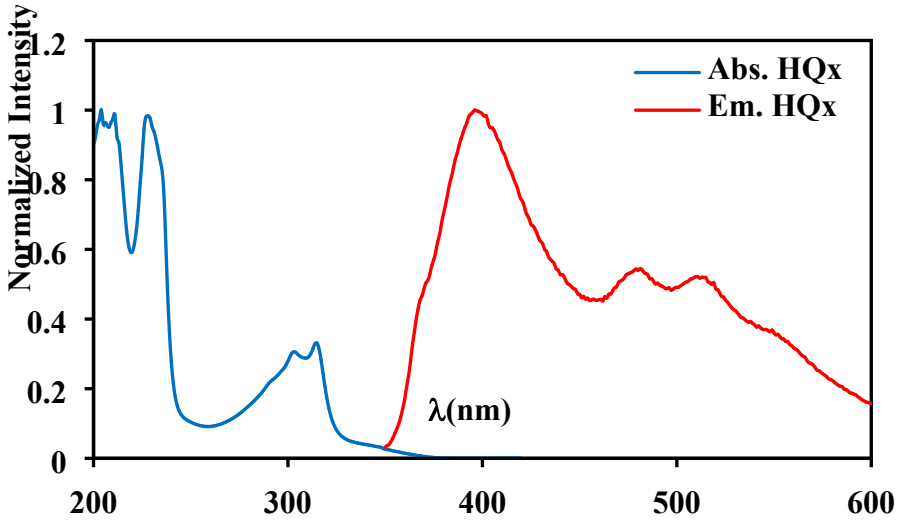

Figure S18. Normalized absorption and emission spectra of **(Qx-H)Cl** recorded in CH_3CN at 298 K.

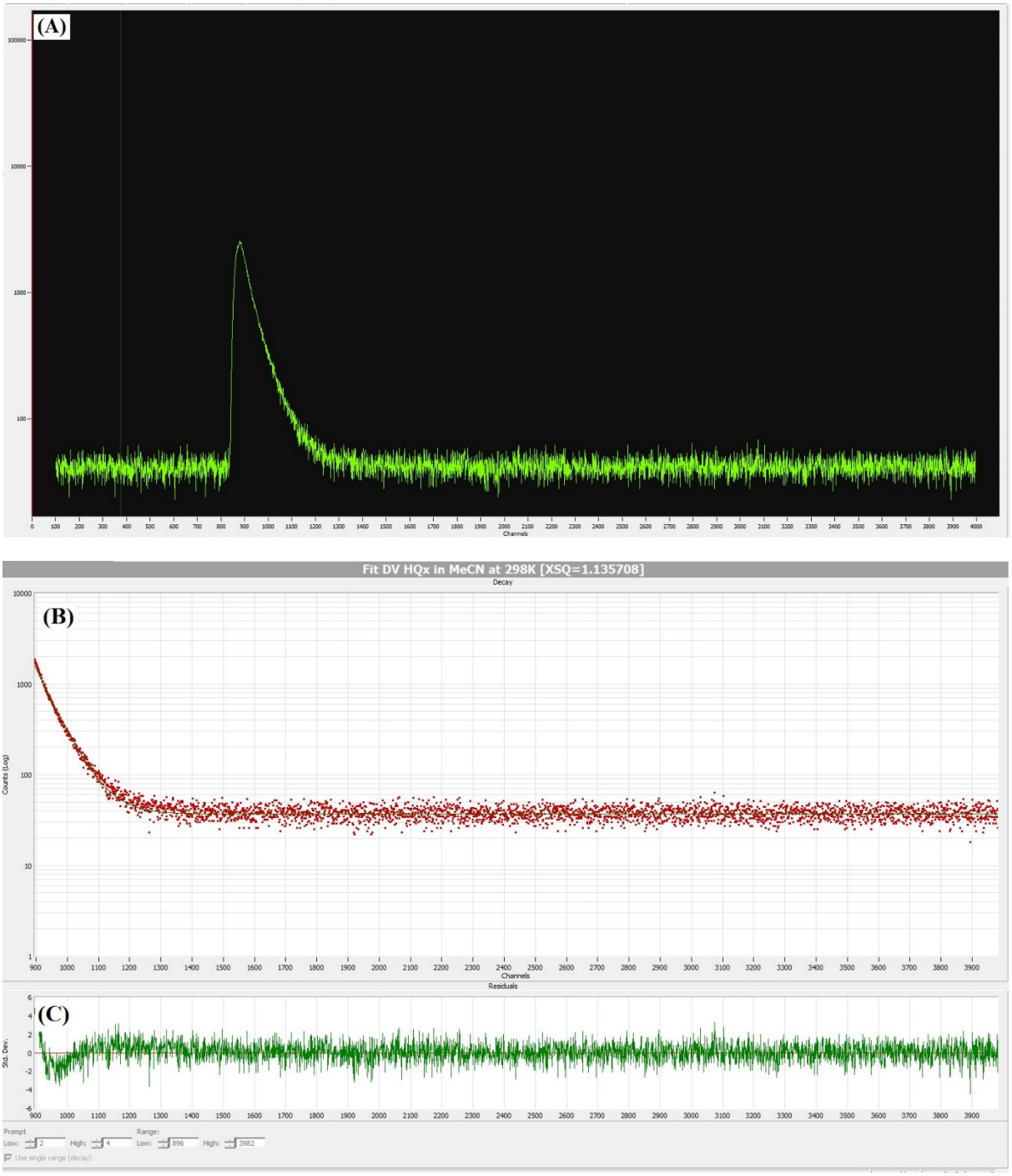

Figure S19. (A) Emission decay, **(B)** best fit and **(C)** residuals of **(Qx-H)Cl** in CH_3CN at rt; $\chi^2 = 1.135$.

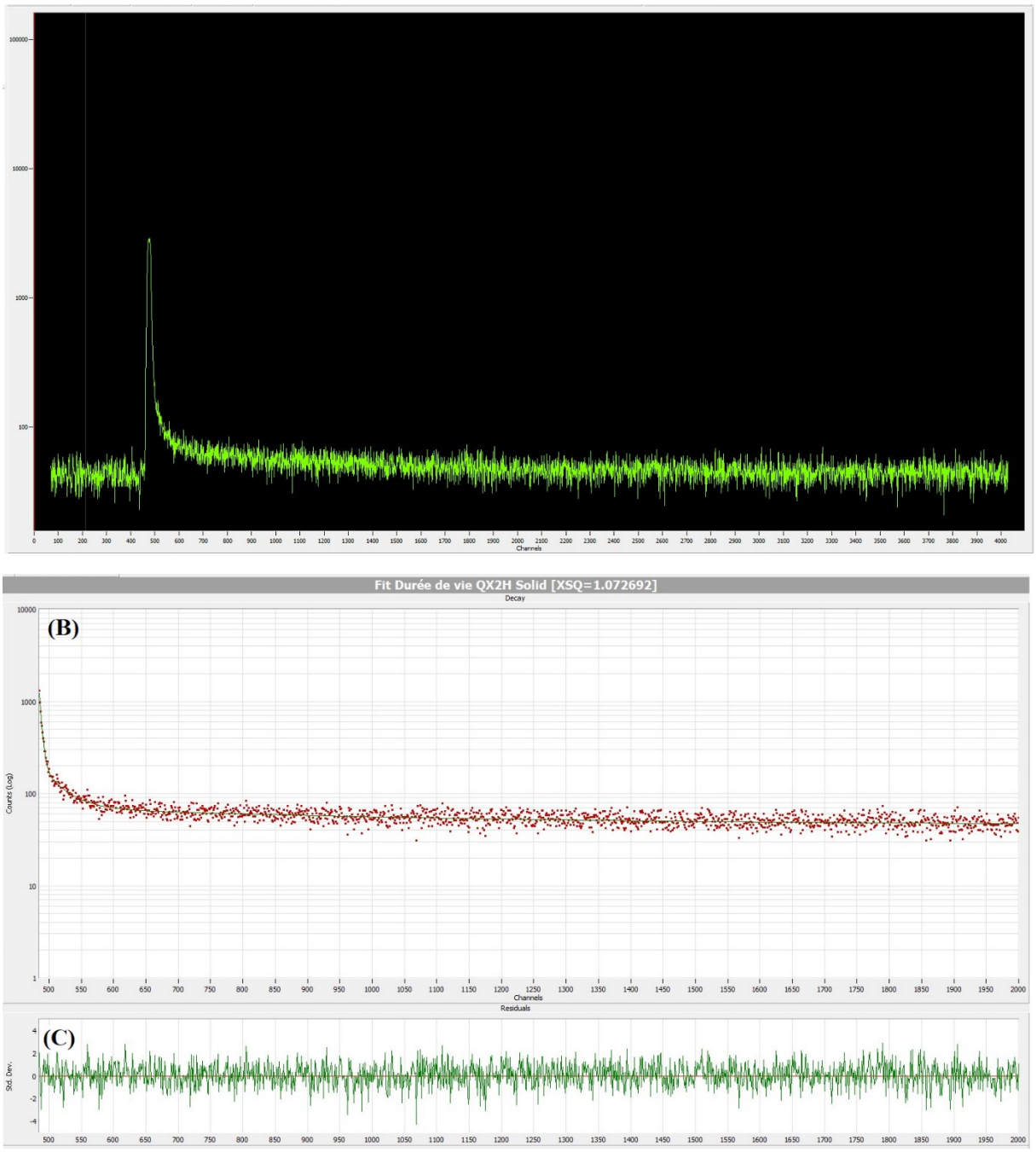

Figure S20. (A) Emission decay, **(B)** best fit and **(C)** residuals of **(Qx-H)Cl** in solid-state at rt; $\chi^2 = 1.072$.

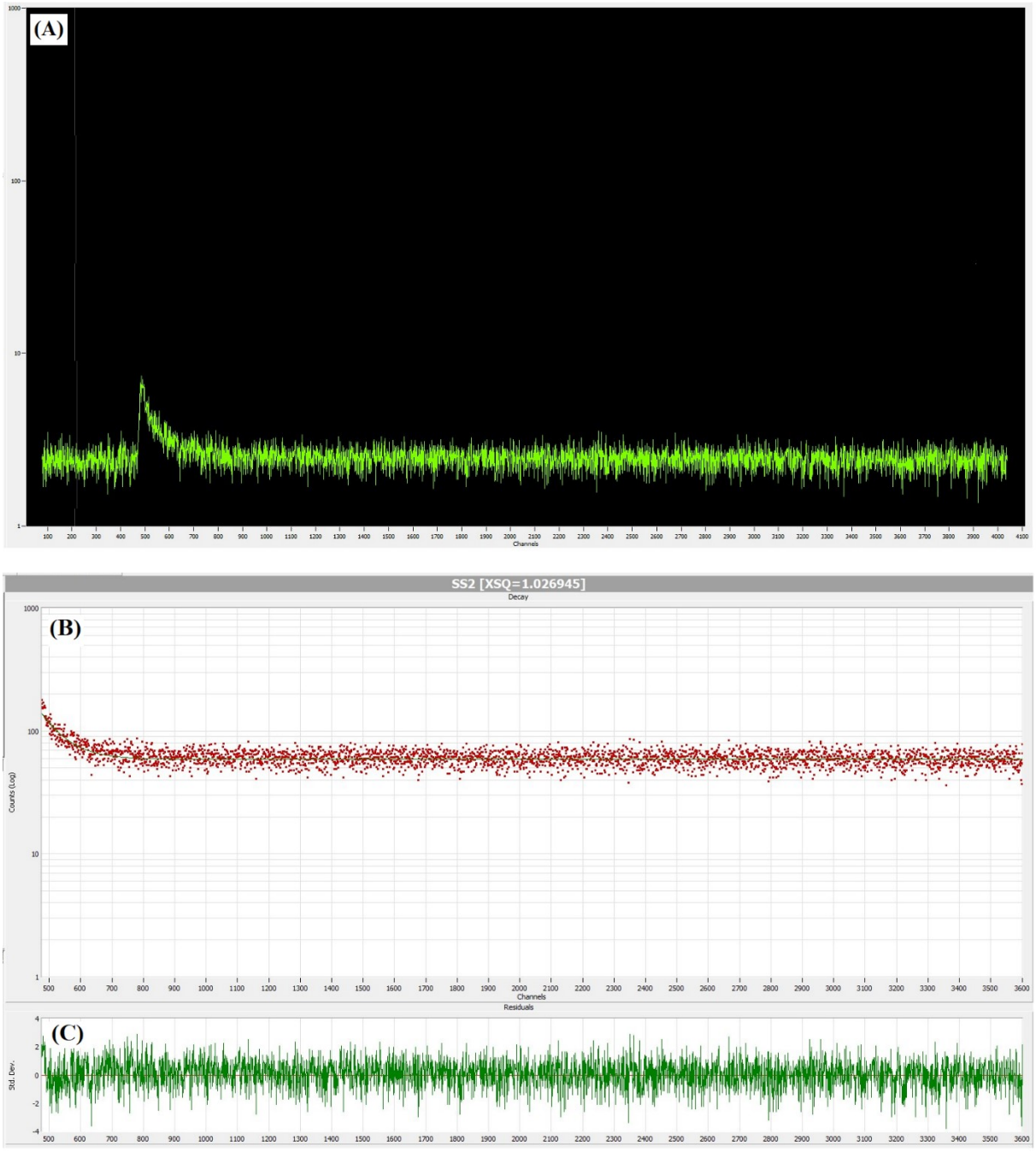

Figure S21. (A) Emission decay, **(B)** best fit and **(C)** residuals of **1** in CH_3CN at rt; $\chi^2 = 1.026$.

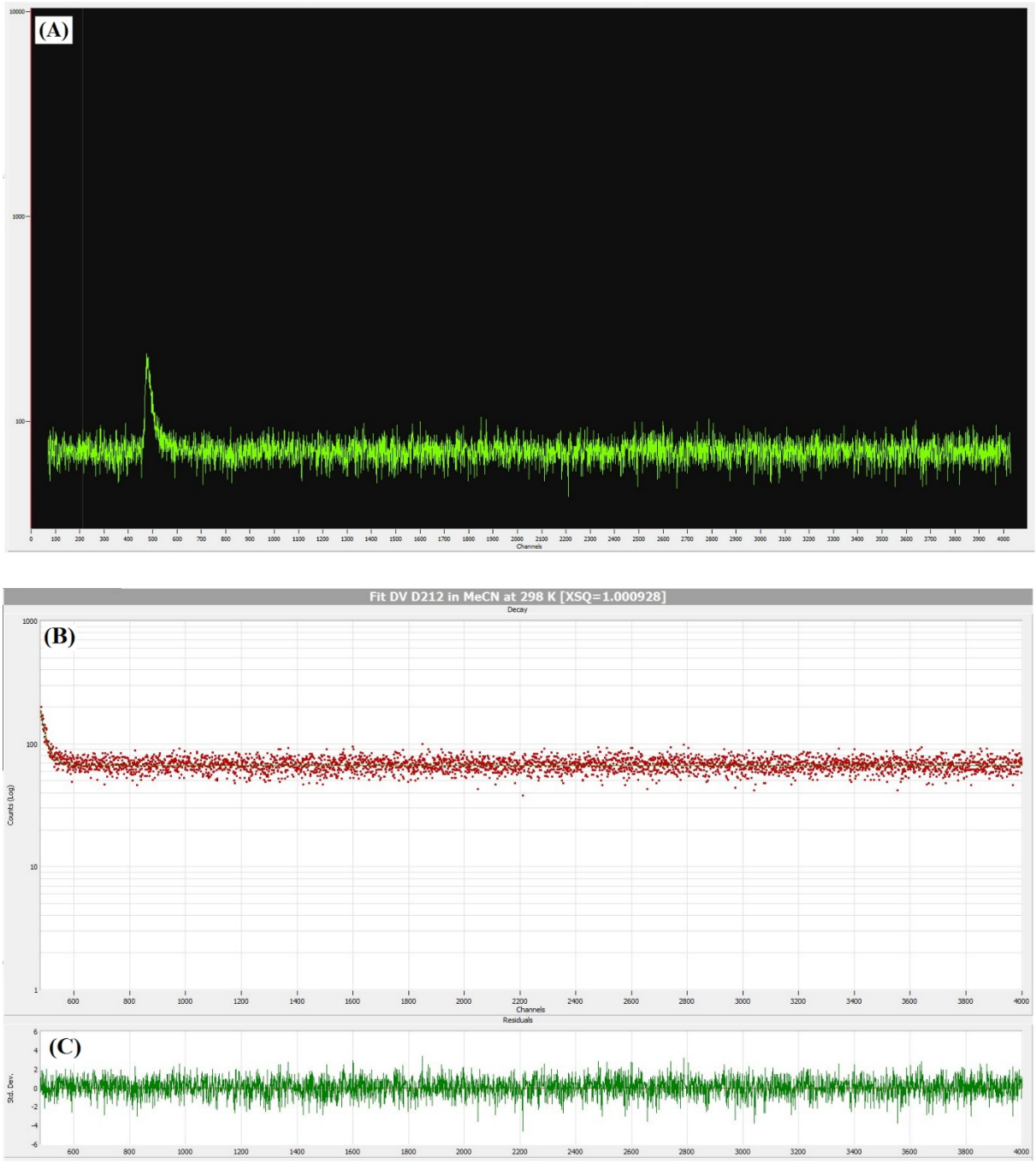

Figure S22. (A) Emission decay, **(B)** best fit and **(C)** residuals of **2** in CH_3CN at rt; $\chi^2 = 1.000$.

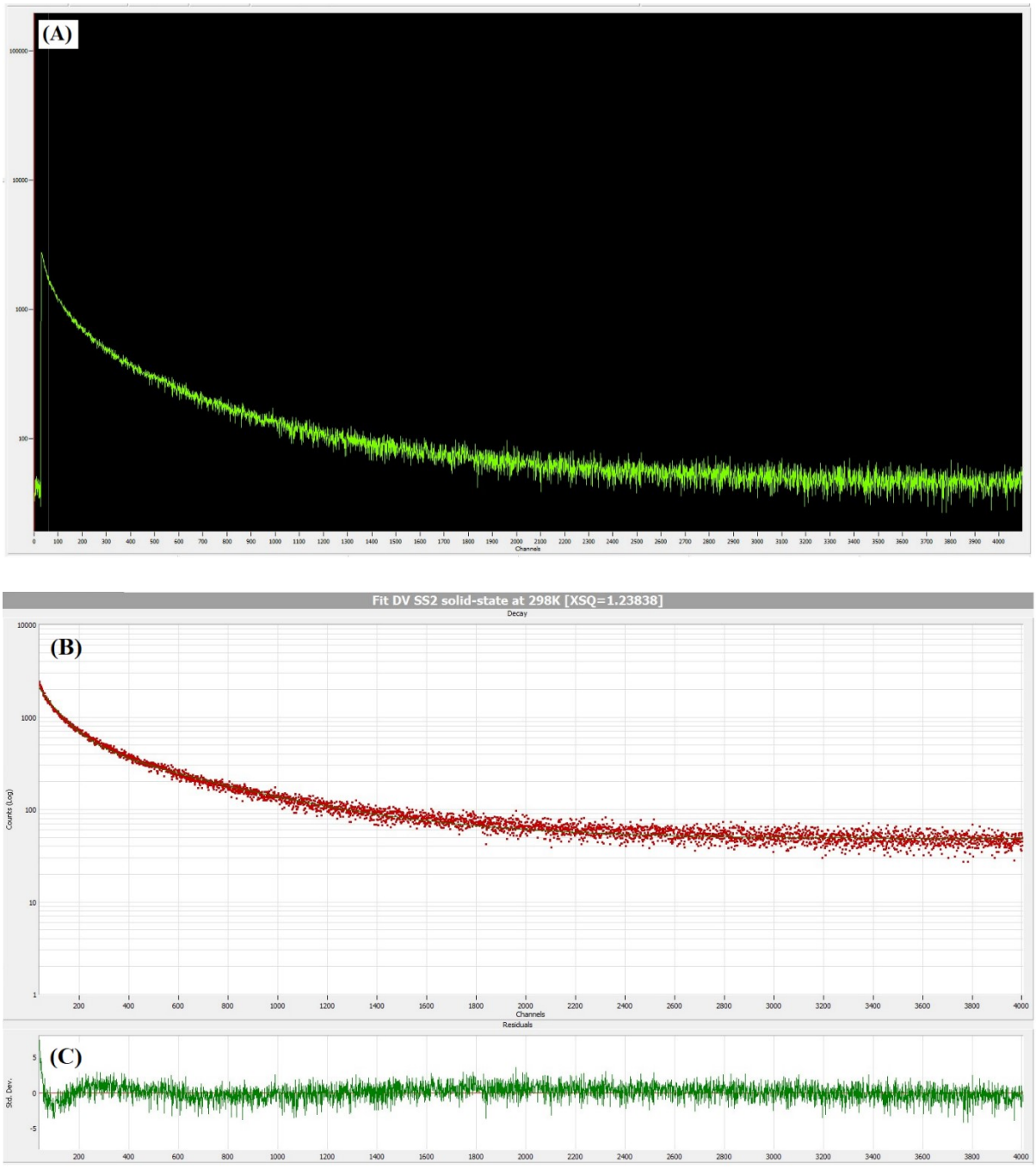

Figure S23. (A) Emission decay, **(B)** best fit and **(C)** residuals of **1** in solid-state at rt; $\chi^2 = 1.238$

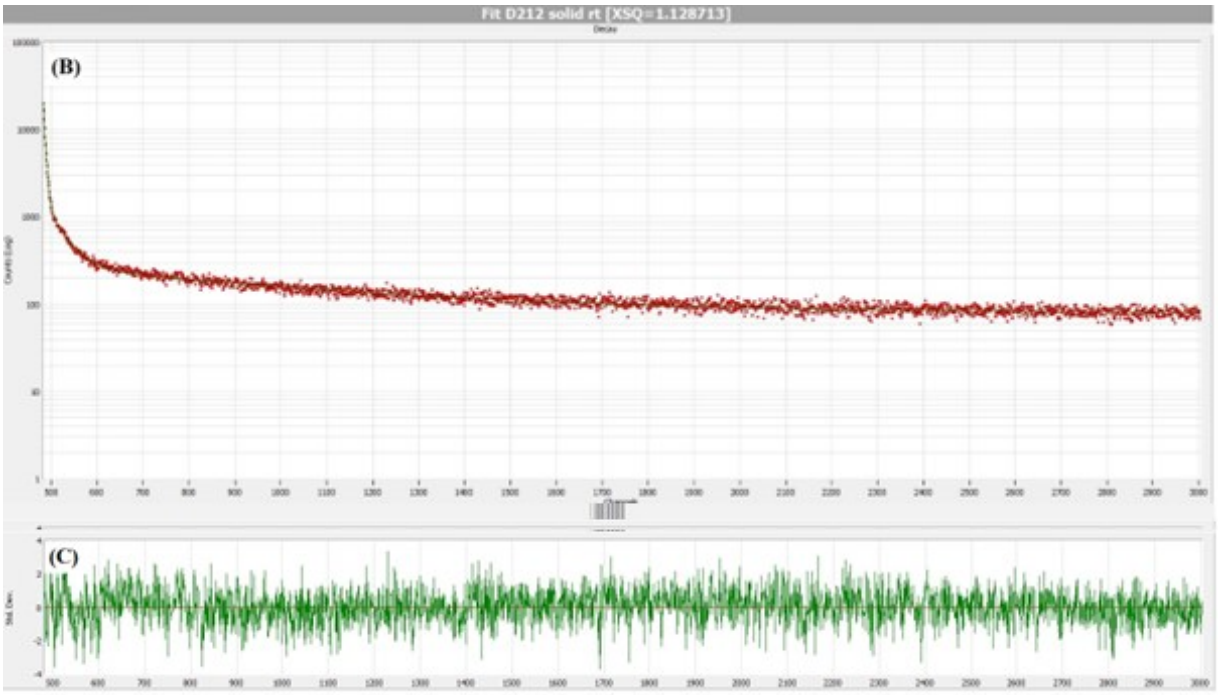

Figure S24. (A) Emission decay, **(B)** best fit and **(C)** residuals of **2** in solid-state at rt; $\chi^2 = 1.128$.

Table S1. Selected interatomic distances (Å) and angles (°) in the (bpy-H^+) cation of **1**.

Bond length (Å)		**Bond angles (°)**	
N1—H1	0.8800	C1—N1—H1	120.9
N1—C1	1.433 (7)	C5—N1—H1	120.9
N1—C5	1.313 (13)	C5—N1—C1	118.3 (6)
N2—C6	1.444 (13)	C10—N2—C6	114.5 (7)
N2—C10	1.302 (13)	N1—C1—H1A	119.5
C1—H1A	0.9500	C2—C1—N1	121.0 (5)
C1—C2	1.389 (7)	C2—C1—H1A	119.5
C2—H2	0.9500	C1—C2—H2	120.0
C2—C3	1.370 (7)	C3—C2—C1	119.9 (5)
C3—H3	0.9500	C3—C2—H2	120.0
C3—C4	1.372 (7)	C2—C3—H3	119.6
C4—H4	0.9500	C2—C3—C4	120.8 (5)
C4—C5	1.476 (15)	C4—C3—H3	119.6
C5—C6	1.479 (4)	C3—C4—H4	121.0
C6—C7	1.279 (13)	N2—C10—H10	116.9
C7—H7	0.9500	C9—C10—H10	116.9
C7—C8	1.397 (11)	N2—C10—C9	126.1 (8)
C8—H8	0.9500	N1—C5—C6	127.6 (11)
C8—C9	1.438 (12)	C4—C5—C6	109.7 (9)
C9—H9	0.9500	N2—C6—C5	114.3 (10)
C9—C10	1.347 (14)	C3—C4—C5	118.1 (5)
C10—H10	0.9500	C5—C4—H4	121.0
		N1—C5—C4	121.1 (5)
		C7—C6—N2	123.6 (3)
		C7—C6—C5	122.1 (10)
		C6—C7—H7	119.6
		C6—C7—C8	120.7 (7)
		C8—C7—H7	119.6
		C7—C8—H8	121.6
		C7—C8—C9	116.8 (7)
		C9—C8—H8	121.6
		C8—C9—H9	121.2
		C10—C9—C8	117.6 (4)
		C10—C9—H9	121.2

Table S2. Hydrogen bonds geometry (Å, °) for the compound **1**.

D—H···*A*	*D*—H	H···*A*	*D*···*A*	*D*—H···*A*
N1—H1···I4^{iii}	0.88	3.23	4.100 (5)	171
C2—H2···I4^{iv}	0.95	3.12	4.034 (6)	163
C4—H4···I1	0.95	2.88	3.673 (5)	142
C7—H7···I4^{iii}	0.95	3.22	4.152 (8)	168
C9—H9···I2^{v}	0.95	3.23	3.942 (7)	134
C9—H9···I3^{v}	0.95	3.11	3.890 (6)	140
C10—H10···I2^{vi}	0.95	3.16	4.082 (9)	164

Symmetry codes: (iii) $x+1, y, z$; (iv) $x+1/2, -y+1/2, z-1/2$; (v) $x+1/2, y+1/2, z$; (vi) $x, -y+1, z-1/2$.

Table S3. Selected interatomic distances (Å) and angles (°) in the (Qx-H$^+$) cation and MeOH of **2**.

Bond length (Å)		**Bond angles (°)**	
O1—H1B	0.8400	C9—O1—H1B	109.5
O1—C9	1.414 (14)	O1—C9—H9A	109.5
C9—H9A	0.9800	O1—C9—H9B	109.5
C9—H9B	0.9800	O1—C9—H9C	109.5
C9—H9C	0.9800	H9A—C9—H9B	109.5
N1—H1	0.8800	H9A—C9—H9C	109.5
N1—C1	1.346 (13)	H9B—C9—H9C	109.5
N1—C8	1.324 (10)	C1—N1—H1	119.6
N2—C6	1.346 (12)	C8—N1—H1	119.6
N2—C7	1.305 (13)	C8—N1—C1	120.7 (7)
C1—C2	1.430 (13)	C7—N2—C6	120.6 (7)
C1—C6	1.421 (9)	N1—C1—C2	118.2 (10)
C2—H2	0.91 (7)	N1—C1—C6	119.1 (8)
C2—C3	1.369 (11)	C6—C1—C2	122.6 (12)
C3—H3	0.9500	C1—C2—H2	122 (5)
C3—C4	1.417 (12)	C3—C2—C1	116.2 (13)
C4—H4	0.97 (6)	C3—C2—H2	121 (5)
C4—C5	1.386 (13)	C2—C3—H3	118.9
C5—H5	0.96 (8)	C2—C3—C4	122.2 (12)
C5—C6	1.415 (10)	C4—C3—H3	118.9
C7—H7	0.96 (8)	C3—C4—H4	116 (4)
C7—C8	1.390 (12)	C5—C4—C3	122.0 (12)
C8—H8	1.03 (7)	C5—C4—H4	122 (4)
N1A—H1A	0.8800	C4—C5—H5	127 (5)
N1A—C1A	1.39 (4)	C4—C5—C6	117.9 (10)

N1A—C8A	1.29 (3)	C6—C5—H5	114 (5)
N2A—C6A	1.47 (3)	N2—C6—C1	118.6 (8)
N2A—C7A	1.29 (2)	N2—C6—C5	122.3 (7)
C1A—C2A	1.39 (3)	C5—C6—C1	119.1 (9)
C1A—C6A	1.37 (3)	N2—C7—H7	122 (5)
C2A—H2A	0.9500	N2—C7—C8	121.4 (7)
C2A—C3A	1.33 (3)	C8—C7—H7	117 (5)
C3A—H3A	0.9500	N1—C8—C7	119.4 (8)
C3A—C4A	1.38 (3)	N1—C8—H8	115 (4)
C4A—H4A	0.9500	C7—C8—H8	125 (4)
C4A—C5A	1.35 (3)	C1A—N1A—H1A	119.7
C5A—H5A	0.9500	C8A—N1A—H1A	119.7
C5A—C6A	1.37 (2)	C8A—N1A—C1A	121 (2)
C7A—H7A	0.9500	C7A—N2A—C6A	115 (2)
C7A—C8A	1.40 (2)	N1A—C1A—C2A	132 (4)
C8A—H8A	0.9500	C6A—C1A—N1A	117 (3)
		C6A—C1A—C2A	111 (4)
		C1A—C2A—H2A	115.8
		C3A—C2A—C1A	128 (5)
		C3A—C2A—H2A	115.8
		C2A—C3A—H3A	120.6
		C2A—C3A—C4A	119 (4)
		C4A—C3A—H3A	120.6
		C3A—C4A—H4A	122.4
		C5A—C4A—C3A	115 (4)
		C5A—C4A—H4A	122.4
		C4A—C5A—H5A	117.7
		C4A—C5A—C6A	125 (3)
		C6A—C5A—H5A	117.7
		C1A—C6A—N2A	122 (2)
		C1A—C6A—C5A	122 (3)
		C5A—C6A—N2A	116 (2)
		N2A—C7A—H7A	118.9
		N2A—C7A—C8A	122.3 (18)
		C8A—C7A—H7A	118.9
		N1A—C8A—C7A	123 (2)
		N1A—C8A—H8A	118.7
		C7A—C8A—H8A	118.7

Table S4. Hydrogen bonds geometry (Å, °) for the compound **2**.

D*—H···*A	***D*—H**	**H···*A***	***D*···*A***	***D*—H···*A***
O1—H1*B*···I2^{iii}	0.84	2.92	3.680 (11)	152
C9—H9A···I2^{iv}	0.98	3.27	4.04 (3)	137
C9—H9A···I3^{iv}	0.98	3.13	3.91 (4)	138
C9—H9B···I3^{iii}	0.98	3.20	3.88 (4)	127
C2A—H2A···I2^{iv}	0.95	3.12	4.05 (5)	165
C7A—H7A···I1	0.95	3.12	3.856 (17)	136
C7A—H7A···I4^{v}	0.95	3.17	3.849 (19)	130
C2—H2···I2^{iv}	0.92 (8)	3.22 (8)	4.039 (17)	149 (6)
C5—H5···I3^{vi}	0.98 (9)	3.23 (9)	4.195 (12)	172 (7)
C7—H7···I1^{v}	0.96 (9)	3.29 (9)	3.784 (19)	114 (6)
C7—H7···I4^{v}	0.96 (9)	3.24 (8)	3.857 (10)	124 (6)
C8—H8···I1	1.03 (7)	3.21 (7)	3.956 (10)	130 (5)
C8—H8···I4^{iii}	1.03 (7)	3.30 (7)	3.816 (12)	112 (4)

Symmetry codes: (iii) $x+1, y, z$; (iv) $-x+1, -y+2, -z$; (v) $-x+1, -y+1, -z+1$; (vi) $x, y-1, z$.

Table S5. Frequencies (cm^{-1}) of the observed Raman and infrared bands of **1** and proposed assignments.

Wavenumber (cm^{-1})		Assignment
Raman	Infrared	
55		Bending modes
77		
88		
95		$Sb–I_{(bridge)}$ stretching
112		
126		
156		$Sb–I_{(external)}$ stretching
	423	γ(heterocyclic ring)
	441	heterocyclic ring torsion
	542	δ(CCC) + δ(CCN)
	610	
	635	
	718	γ(C=C) + γ(C=N)
	737	
	761	γ(C–H)aromatic
	811	
	935	
	998	β(C–H)aromatic
	1008	
	1035	
	1063	
	1081	
	1153	
	1166	
	1209	
	1249	ν(C=C)+ν(C=N)
	1349	
	1427	
	1451	
	1465	
	1520	
	1578	
	1594	
	1612	
	2887	ν(C–H)aromatic
	2930	
	2974	
	3043	
	3081	
	3205	$ν(NH^+)$
	3250	

ν: stretching, δ: deformation, β: in plane bending, γ: out of plane bending

Table S6. Frequencies (cm^{-1}) of the observed Raman and infrared bands of **2** and proposed assignments.

Wavenumber (cm^{-1})		Assignment
Raman	Infrared	
55		Bending modes
73		
93		$Bi–I_{(bridge)}$ stretching
122		
141		$Bi–I_{(external)}$ stretching
	453	δ(CCC)
	472	
	524	δ(CCN)
	600	
	756	γ(C=C) + γ(C=N)
	799	
	844	
	869	
	906	γ(CCH)aromatic
	943	
	970	
	1037	ν(C–O)methanol
	1071	
	1129	δ(CCH)aromatic
	1141	
	1184	
	1218	
	1245	
	1334	ν(C=C)
	1352	
	1395	
	1459	
	1517	
	1566	$\nu(C=NH^+)$
	1603	
	1615	
	3026	ν(C–H)methanol
	3063	
	3125	ν(C–H)aromatic
	3155	
	3197	$\nu(NH^+)$
	3234	
	3455	ν(O–H)methanol

References

1 M. D. Petrov, M. N. Sokolov, V. P. Fedin and S. A. Adonin, *J. Struct. Chem*., 2020, **61**, 1794-1799. https://doi.org/10.1134/S0022476620110128.

2 A. Lipka*, Zeitschrift für Naturforschung B*, 1983, **38**, 1615–1621. https://doi.org/10.1515/znb-1983-1213.